Organic Electronics 15 (2014) 2885–2892

Contents lists available at ScienceDirect

Organic Electronics

journal homepage: www.elsevier.com/locate/orgel

Effects of incorporating salts with various alkyl chain lengths on carrier balance of light-emitting electrochemical cells

Ray Sun, Chih-Teng Liao, Hai-Ching Su *

Institute of Lighting and Energy Photonics, National Chiao Tung University, Tainan 71150, Taiwan

ARTICLE INFO

Article history:
Received 18 April 2014
Received in revised form 15 August 2014
Accepted 15 August 2014
Available online 28 August 2014

Keywords:
Light-emitting electrochemical cells
Salts
Carrier balance

ABSTRACT

Recently, solid-state light-emitting electrochemical cells (LECs) have attracted much attention since they have advantages such as low operation voltages, simple device structure and balanced carrier injection. Salts are commonly added in the emissive layer of LECs to provide additional mobile ions and thus to accelerate device response. However, in addition to modified ionic property, carrier balance of LECs would also be tailored by salt additives. In this work, we improve device efficiency of LECs by incorporating imidazole-based salts bearing various alkyl chain lengths. As the alkyl chain length of the added salt increases, the device current decreases and the recombination zone approaches the anode. These results reveal that hole transport in the emissive layer of LEC containing a salt with a larger size would be impeded more significantly than electron transport. When doped with a salt possessing a proper size, nearly doubled device efficiency as compared to that of the neat-film device can be obtained due to improved carrier balance. This work demonstrates a feasible strategy to improve device performance of LECs and clarifies the physical insights of the effect of salt size on carrier balance of LECs.

1. Introduction

As compared to conventional organic light-emitting diodes (OLEDs), which have been shown to exhibit great potential in displays and solid-state lighting, solid-state light-emitting electrochemical cells (LECs) possess several further advantages. In the emissive layer of LECs, electrochemically doped regions induced by spatially separated mobile ions under a bias form ohmic contacts with electrodes, giving balanced carrier injection, low operating voltages and consequently high power efficiencies [1,2]. Hence, only a single emissive layer, which can be easily processed from solutions, is generally required in LECs. In addition, air-stable electrodes, e.g. Au and Ag can be used in LECs due to facilitated carrier injection by doped regions while OLEDs typically require more sophisticated multilayer structures and low-work-function cathodes [3]. The emissive-layer materials of LECs can be categorized into two types: conjugated polymers and cationic transition metal complexes (CTMCs). Polymer LECs are usually composed of an emissive conjugated polymer, a salt and an ion-conducting polymer to avoid phase separation [1,2]. However, for LECs based on CTMCs, no ion-conducting material is needed since these metal complexes are intrinsically ionic. Furthermore, higher electroluminescent (EL) efficiencies are expected due to the phosphorescent nature of the metal complexes. Owing to these advantages, LECs based on CTMCs have attracted much attention in recent years [4–26]. Efficient blue [20,23], green [9,14], yellow [11] and white-emitting [25] CTMC-based LECs have been reported to show high external quantum efficiencies (EQEs) >10%.

Ionic salts have been commonly added in the emissive layer of LECs to improve device performance [27–29].

* Corresponding author. Tel.: +886 6 3032121 57792; fax: +886 6 3032535.
E-mail address: haichingsu@mail.nctu.edu.tw (H.-C. Su).

http://dx.doi.org/10.1016/j.orgel.2014.08.031
1566-1199/

Additional mobile ions provided by the salt additives can reduce the time required for the formation of the doped layers, fastening the device response [27–29]. Furthermore, the device efficiencies of polymer LECs were shown to be dependent on the cation size of the added salts [30]. The emission zone position in the emissive layer of planar polymer LECs have also been shown to be related to the cation size of the added salts [30]. A recent literature depicted that interfacial packing of salt cations at the cathode of CTMC-based LECs enhances electron injection efficiency, resulting in more balanced hole and electron concentrations [29]. These results indicate that the salt additives not only affect the ionic mobility and doping propagation speed but also alter the carrier balance of LECs. To optimize device efficiencies of LECs, overall carrier balance including carrier injection and transport should be considered. However, few reports concerning detailed effects of varying the molecular size of the added salts on carrier balance of sandwich LECs have been published [30,31]. In this work, several imidazole-based salts containing various alkyl chain lengths are incorporated in the emissive layer of CTMC-based LECs and their device characteristics are compared. The device current monotonically decreases as the alkyl chain length of the salt increases since a lager salt molecule increases the intermolecular distance between the emissive complexes and impedes carrier transport. In spite of decreased device current, the device efficiency in the LECs doped with salts is improved as compared to the neat-film devices. The trend of device efficiency versus the alkyl chain length of the salt corresponds to the recombination zone position in the LEC device. More centered recombination zone in the emissive layer suffers less degree of exciton quenching and leads to a higher device efficiency consequently. These results demonstrate a feasible way to optimize the carrier balance of LECs by doping a salt with a proper alkyl chain length.

2. Experiment section

2.1. Materials

The host complex (**1**) used in the emissive layer of the LECs was $Ru(dtb\text{-}bpy)_3(PF_6)_2$ (where dtb-bpy is 4,4′-ditertbutyl-2,2′-bipyridine) [5]. Complex **1** was purchased from Luminescence Technology. The salts used in this study were 1-ethyl-3-methylimidazolium hexafluorophosphate ($EMIMPF_6$), 1-butyl-3-methylimidazolium hexafluorophosphate ($BMIMPF_6$), 1-hexyl-3-methylimidazolium hexafluorophosphate ($HMIMPF_6$) and 1-octyl-3-methylimidazolium hexafluorophosphate ($OMIMPF_6$). $OMIMPF_6$ was purchased from Tokyo Chemical Industry and the other salts were purchased from Alfa Aesar. All materials were used as received.

2.2. LEC device fabrication and characterization

Indium tin oxide (ITO)-coated glass substrates were cleaned and treated with UV/ozone prior to use. A thin poly(3,4-ethylenedioxythiophene):poly(styrene sulfonate) (PEDOT:PSS) layer (30 nm) was spin-coated at 4000 rpm onto the ITO substrate in air and was then baked at 150 °C for 30 min. For the thinner devices (**N1**, **E1**, **B1**, **H1** and **O1**), the emissive layers were then spin-coated at 3000 rpm from the acetonitrile solutions of complex **1** or complex **1** and salts (80 mg mL^{-1}). The emissive layer of the device **N1** was composed of a neat film of complex **1** while those of the devices **E1**, **B1**, **H1** and **O1** contained complex **1** doped with $EMIMPF_6$, $BMIMPF_6$, $HMIMPF_6$ and $OMIMPF_6$, respectively (molar ratio of complex **1** and salt = 2.1: 1). For the thicker devices (**N2**, **E2**, **B2**, **H2** and **O2**), the concentrations of the solutions used for spin coating of the emissive layers were 250 mg mL^{-1}. The rotation speed for spin coating and the components of the emissive layers of the thicker devices were the same with those used for their thinner counterparts. The thicknesses of the thinner and thicker devices were measured by ellipsometry to be ca. 250 and 600 nm, respectively. After spin coating of the emissive layers, the samples were then baked at 70 °C for 10 h in a nitrogen glove box, followed by thermal evaporation of a 100-nm Ag top contact in a vacuum chamber ($\sim 10^{-6}$ torr). The electrical and emission characteristics of LEC devices were measured using a source-measurement unit and a calibrated Si photodiode. All device measurements were performed under constant bias voltages in a nitrogen glove box. The EL spectra were taken with a calibrated CCD spectrograph.

3. Results and discussions

The molecular structures of the salts used in this study are shown in Fig. 1. The alkyl chain length increases in the order; $EMIMPF_6$, $BMIMPF_6$, $HMIMPF_6$ and $OMIMPF_6$. The physical properties of the salts used in this study are summarized in Table 1. The volume per molecule of each salt was calculated from the molar mass and density data [32–34]. The molecular volume of the salt increases with the alkyl chain length since a longer alkyl chain occupies more space. When doped in the emissive layer of LECs, the salt molecules tend to increase the intermolecular distance between the emissive complexes. As shown in Fig. 2,

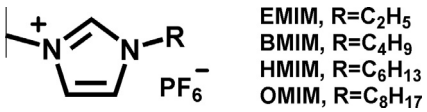

Fig. 1. Molecular structures of the salts used in this study.

Table 1
Summary of the physical properties of the salts used in this study.

Salt	Molar mass (g mol^{-1})	Density (g cm^{-3})[a]	Volume per molecule (nm^3)[b]
$EMIMPF_6$	256.13	1.56[c]	0.274
$BMIMPF_6$	284.18	1.37[d]	0.346
$HMIMPF_6$	312.24	1.29[e]	0.403
$OMIMPF_6$	340.29	1.24[d]	0.457

[a] At 298 K.
[b] Calculated from molar mass and density data.
[c] Ref. [31].
[d] Ref. [32].
[e] Ref. [33].

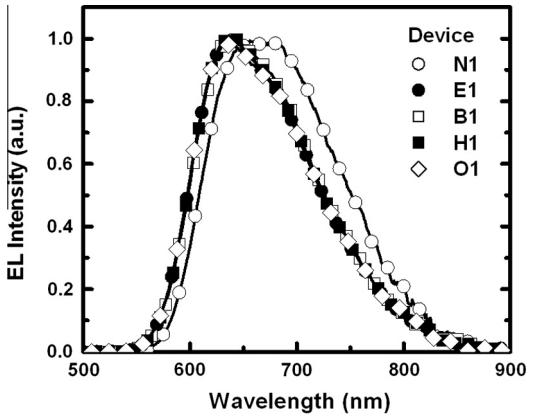

Fig. 2. The EL spectra of the LEC devices **N1**, **E1**, **B1**, **H1** and **O1** under 2.6 V.

the neat-film device (**N1**) showed an EL emission peak at ca. 660 nm while the EL of the devices containing salts (**E1**, **B1**, **H1** and **O1**) centered at ca. 640 nm. Such blue-shifted EL emission confirms reduced intermolecular interactions induced by the added salts.

To study the effects of adding salts on carrier balance, the EL characteristics of LECs without and with salts were measured and are summarized in Table 2. Comparison of device current would clarify the impact of the salt additive on carrier injection and transport properties of the devices. As shown in Fig. 3, the device current first increased with time and reached a plateau value finally. When a bias was applied, the mobile ions drifted toward electrodes and the doped layers were formed gradually. Carrier injection efficiencies were enhanced due to formation of the doped layers and the device current increased consequently. It is noted that the device current densities decreased with increasing alkyl chain length of the added salts. A recent study indicated that ohmic contacts at electrodes of LECs based on CTMCs can be achieved only when the carrier injection barrier is relatively low [23]. For a relatively larger carrier injection barrier (ca. 1 eV), some residual barrier is still present even when the doped regions have been formed. As a result, strategies to enhance carrier injection, e.g. inserting carrier injection layer at electrodes, can increase device current substantially [23]. The work functions of electrodes and energy levels of complex **1** are depicted in Fig. 4 [35]. The hole injection barrier at the anode is only 0.42 eV while the electron injection barrier is up to 1.03 eV. The salts provided additional mobile ions, which can accumulate at the electrodes under a bias and increase the doping concentrations, rendering enhanced carrier injection efficiencies [29]. Improving injection efficiency by adding salts would be more significant for electrons since a much larger potential barrier is present at the cathode. Therefore, when these salts were added, device currents should increase due to enhanced carrier injection. However, reduced device currents were measured instead for all LECs with salts (Fig. 3). Such phenomenon may be rationally attributed to impeded carrier transport induced by the salts. The salt molecules isolated the emissive complexes and thus it would be more difficult for carriers to hop between complexes under an applied electric field. Reduced carrier mobilities decreased device current densities consequently. Increased device currents due to enhanced carrier injection can not compensate for decreased device currents resulted from impeded carrier transport, rendering reduced device current densities of LECs containing salts. Larger salt molecules resulted in lower device currents since longer intermolecular distances between complexes reduced carrier mobilities more significantly. It implies that carrier balance of LECs can be adjusted by varying the alkyl chain length of the added salts.

Table 2
Summary of the LEC device characteristics.

Device	Bias (V)	t_{max} (min)[a]	J_{max} (mA cm^{-2})[b]	L_{max} (μW cm^{-2})[c]	$\eta_{ext,max}$ (%)[d]
N2	2.5	41	0.35	9.0	1.84
E2	2.5	57	0.19	5.0	2.55
B2	2.5	36	0.18	5.5	3.27
H2	2.5	62	0.12	3.6	3.15
O2	2.5	115	0.08	2.0	2.40

[a] Time required to reach half of the maximal light output (before reaching the maximal light output).
[b] Maximal current density achieved at a constant bias voltage.
[c] Maximal light output achieved at a constant bias voltage.
[d] Maximal external quantum efficiency achieved at a constant bias voltage.

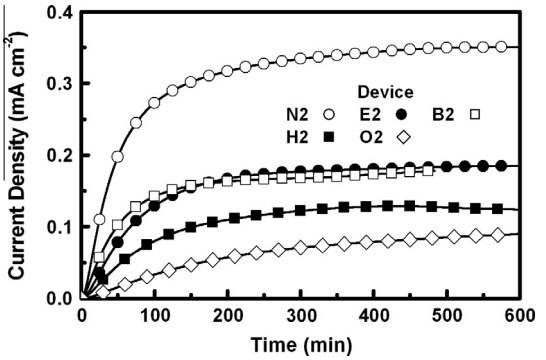

Fig. 3. Current density as a function of time for the LEC devices **N2**, **E2**, **B2**, **H2** and **O2**.

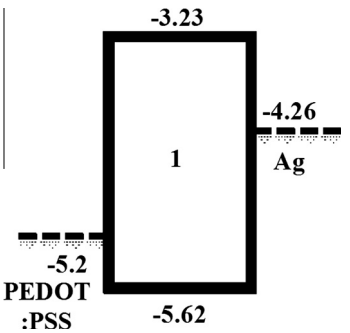

Fig. 4. Work functions of the electrodes and the energy levels of complex **1**.

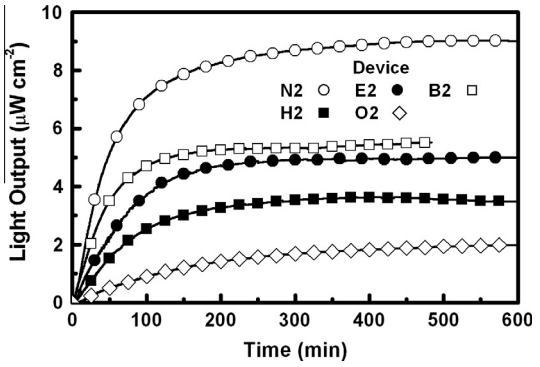

Fig. 5. Light outputs as a function of time for the LEC devices **N2**, **E2**, **B2**, **H2** and **O2**.

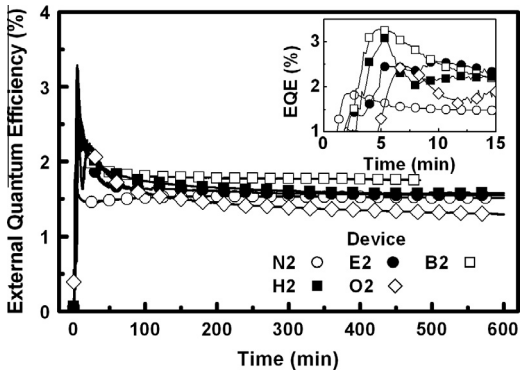

Fig. 6. External quantum efficiency as a function of time for the LEC devices **N2**, **E2**, **B2**, **H2** and **O2**. Inset: magnification of the time-dependent EQE during the first 15-min measurement.

The time-dependent light outputs of LECs without and with salts are shown in Fig. 5. The light outputs first increased with the current and reached the maxima values. All devices exhibited stable current finally and thus degradation would not be significant during 10-h operation. Time-dependent EQEs of the LEC devices without and with salts are depicted in Fig. 6. When a bias was just applied, the EQE was low due to poor carrier injection (Fig. 4). During the formation of the doped layers near electrodes, the carrier injection efficiency was improved and the EQE thus rose rapidly. After reaching the peak value, the EQE decreased with time due to exciton quenching induced by the extension of the doped layers. Furthermore, the degradation of the emissive material during the LEC operation was also responsible for decreased EQEs [36,37]. The EQEs of devices **N2**, **E2**, **B2**, **H2** and **O2** reached steady-state values after 250, 250, 250, 300 and 450 min, respectively (Fig. 6). The current densities of devices **N2**, **E2**, **B2**, **H2** and **O2** at 250, 250, 250, 300 and 450 min were up to 93, 93, 93, 96 and 93%, respectively, of their maximal values. When the device current was almost reaching the maximal value, the doped layers were nearly stabilized and thus the degree of exciton quenching was approximately constant, leading to steady-state EQEs as well. Similar results correlating the time for stabilized doped layers and EQEs of LECs based on the same complex have been reported in Ref. [35]. All LECs doped with salts showed higher peak EQEs than the neat-film devices (Table 2). The peak EQEs increased when an ethyl chain of the added salt was replaced by a butyl chain (cf. device **E2** and **B2**, Table 2). However, further increasing the alkyl chain length of the salt resulted in reduced EQEs (cf. device **H2** and O**2**, Table 2). These data suggest that device efficiency of LECs can be optimized by doping a salt with a proper molecular size.

To further clarify the physical insights of the effect of molecular size of the added salts on device efficiency of LECs, the recombination zone position in the emissive layer should be examined. In our previous study, time-dependent EL spectra induced by microcavity effect were employed to estimate the temporal evolution of recombination zone in sandwich LECs [35]. A similar technique is adopted in this study to compare the recombination zone positions of the LECs doped with different salts. The emission properties of the emissive layer can be modified in a microcavity structure and the output EL spectrum of a bottom emitting OLED device can be calculated approximately by using the following equation [38]:

$$|E_{ext}(\lambda)|^2 = \frac{T_2 \frac{1}{N}\sum_{i=1}^{N}\left[1 + R_1 + 2\sqrt{R_1}\cos\left(\frac{4\pi z_i}{\lambda} + \varphi_1\right)\right]}{1 + R_1R_2 - 2\sqrt{R_1R_2}\cos\left(\frac{4\pi L}{\lambda} + \varphi_1 + \varphi_2\right)} \times |E_{int}(\lambda)|^2$$

where R_1 and R_2 are the reflectance from the cathode and from the glass substrate, respectively, φ_1 and φ_2 are the phase changes on reflection from the cathode and from the glass substrate, respectively, T_2 is the transmittance from the glass substrate, L is the total optical thickness of the cavity layers, $|E_{int}(\lambda)|^2$ is the emission spectrum of the organic materials without alternation of the microcavity effect, $|E_{ext}(\lambda)|^2$ is the output emission spectrum from the glass substrate, z_i is the optical distance between the emitting sublayer i and the cathode. The emitting layer is divided into N sublayers (thickness of each sublayer is 1 nm) and their contributions are summed up. The thickness of the emitting layer is estimated to be ca. 10% of the active-layer thickness according to the measured width of p–n junction in capacitance measurements [39]. To facilitate measurements of time-dependent EL spectra, the thickness of the emissive layer of LECs was chosen to be 600 nm. In thinner LECs, the spectral spacing between the cavity modes, at which constructive interference occurs, is larger and thus the cavity modes are more likely to occur outside the emission spectrum of complex **1**, rendering insignificant shift of EL with time. To fairly correlate the estimated recombination zones with the EL characteristics of the thicker LECs, devices with the same thickness should be used in the optical fitting. Furthermore, carrier balance of the thick and thin LECs would be different since the electric field is significantly higher in thinner devices. The photoluminescence (PL) spectrum of a thin film (600 nm) of the emissive layer coated on a quartz substrate was used as the emission spectrum without alternation of the microcavity effect since no highly reflective metal layer is present in this sample. Based on this simulation technique, the temporal recombination zone position of LECs can be estimated by fitting measured EL spectra to simulated EL spectra with proper emitting layer position.

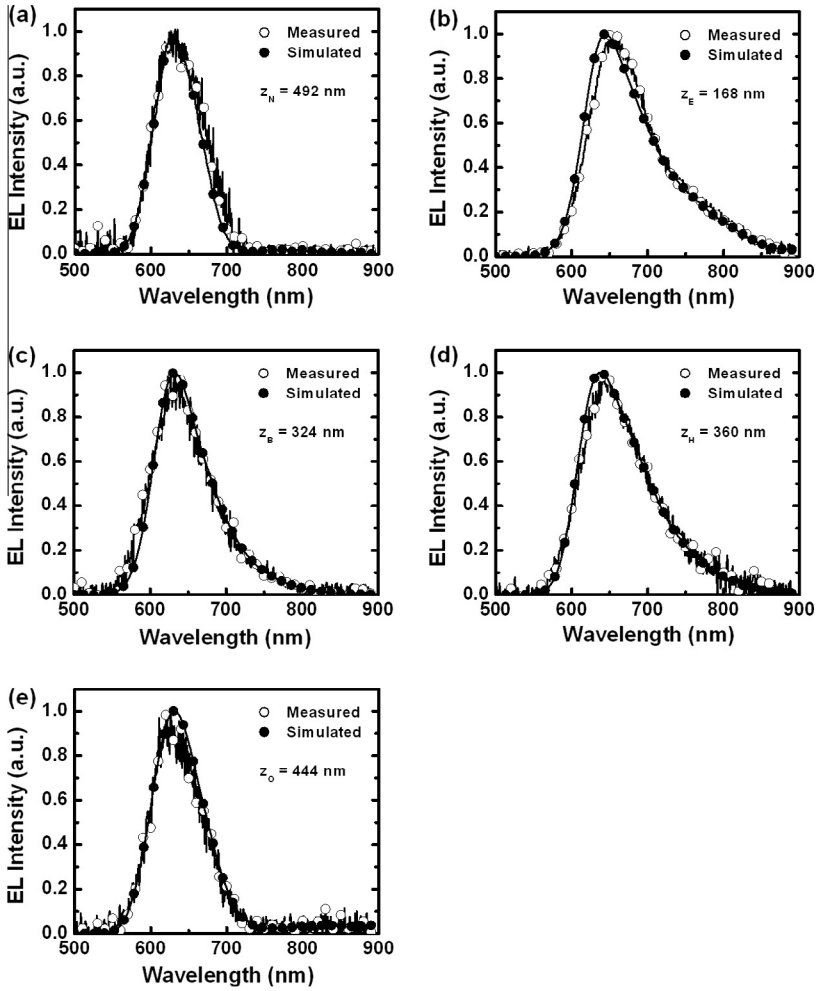

Fig. 7. Simulated (solid symbol) and measured (open symbol) EL spectra when the EQE reached the maximum for devices (a) **N2**, (b) **E2**, (c) **B2**, (d) **H2** and (e) **O2** under 2.5 V. The extracted recombination zone position, as measured from the cathode, of each device is shown on the corresponding subfigure.

The recombination zone positions of these LECs were estimated by utilizing the technique mentioned above. The EL spectrum of each device varied with time due to altered microcavity effect induced by the moving of recombination zone. Fitting of the simulated and measured EL spectra when the EQE reached the maximum for the devices **N2**, **E2**, **B2**, **H2** and **O2** are shown in Fig. 7a–e, respectively. Different shape of the EL spectrum from individual device resulted from different recombination zone position in each device, which affects the wavelength-dependent outcoupling efficiency. The extracted recombination zone position, as measured from the cathode, of each device is shown on the corresponding subfigure. The recombination zone positions of these LECs reflect their peak EQEs. Devices **B2** and **H2** exhibited relatively centered recombination zones and thus they showed high EQEs >3% (Table 2). The recombination zone of device **E2** was close to the cathode while that of device **O2** was close to the anode. Both devices suffered more severe exciton quenching near the doped layers and showed lower EQEs (Table 2). Neat-film device **N2** had the most off-centered recombination zone, which is approaching the anode, rendering the lowest EQE <2% (Table 2). These results confirm that the device efficiency of LECs is strongly dependent on the recombination zone position in the emissive layer. Furthermore, the EL spectra also determined the unit used for light output of the device. As shown in Fig. 7a–e, significant spectral change due to moving of the recombination zone took place at λ = 700–800 nm. EL emission at this spectral range has little contribution to candela values since human eyes are insensitive to the near infrared light. If the unit of brightness (cd. m^{-2}) was used, some EL emission at this spectral range would be underestimated. To accurately calculate the light output, the unit of general power density ($\mu W\ cm^{-2}$) was used instead.

Since the maximum EQE of these LECs reached shortly after the bias was applied (Fig. 6), further extension of the doped layers under a bias resulted in moving of the recombination zone. Temporal evolution of the recombination zone for devices **N2**, **E2**, **B2**, **H2** and **O2** are shown in Fig. 8a–e, respectively. Device containing salts (**E2**, **B2**, **H2** and **O2**) exhibited the same trend in temporal evolution

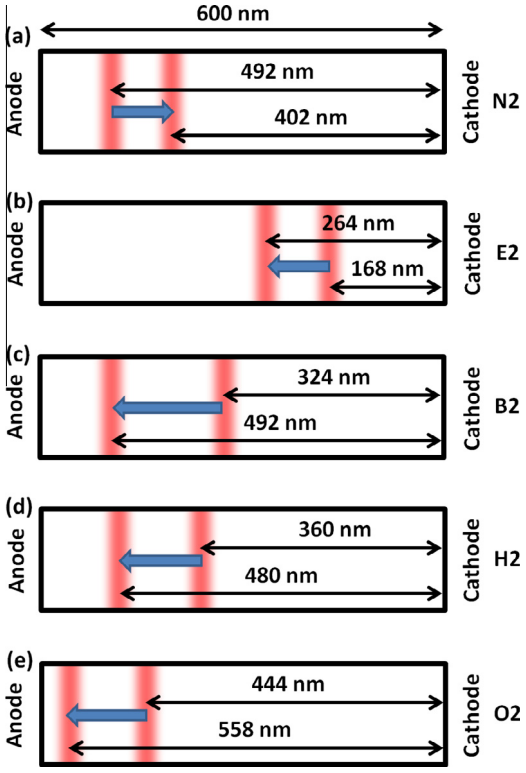

Fig. 8. Temporal evolution of the recombination zone for devices (a) **N2**, (b) **E2**, (c) **B2**, (d) **H2** and (e) **O2**.

of the recombination zone, i.e. moving toward the anode. Such trend of temporal evolution in recombination zone position could be understood by the energy level alignments shown in Fig. 4. The injection barrier for hole (0.42 eV) is much lower than that for electron (1.03 eV). After a bias was just applied, the required amount of accumulated ions near the anode to achieve ohmic contact for hole is smaller than that required to achieve ohmic contact for electron at the cathode. Therefore, the hole injection efficiency was higher at the early stage of formation of the doped layers and the recombination zone would thus locate relatively closer to the cathode initially. When both p- and n-type doped layers were getting well established, carrier injection would approach balanced and thus the recombination zone would move toward the anode with time. It is noted that the recombination zone was closer to the anode as the alkyl chain length of the added salt is longer (cf. Fig. 8b–e). Since incorporating salts in the emissive layer lead to reduction in device current, shifting of the recombination zone due to increasing molecular size of the added salt would be attributed to modified carrier mobilities. Ruthenium complexes containing bipyridyl ligands were shown to exhibit higher electron mobilities than hole mobilities [40]. Furthermore, imidazolium-substituted conjugated polyelectrolytes were introduced as electron transport materials [41]. Hence, incorporating salts with imidazole cores in complex **1** may not affect electron transport significantly. On the other hand, hopping of holes in a complex **1** film blended with electron-transporting salts would be impeded due to increased intermolecular distances. Larger salts resulted in increased intermolecular distances and thus reduced hole mobilities, rendering recombination zones approaching the anode. It is interesting to note that neat-film device **N2** showed a recombination zone closer to the anode and the temporal evolution of recombination zone was reversed as compared to that of devices with salts (Fig. 8a). Compared with devices with salts, neat-film devices contain fewer mobile ions and thus the intrinsic layer between the doped layers would be thicker [42], especially at the early stage of operation. As the intrinsic layer shrank with time due to extension of the doped layers [19,42], field-dependent carrier mobilities would alter the recombination zone positions. The electron mobilities of ruthenium complexes containing bipyridyl ligands were shown to decrease with increasing electric field [40]. Reduction of the intrinsic layer during operation lead to increased electric filed and decreased electron mobility consequently. Therefore, the recombination zone of device **N2** was initially close to the anode and moved to the center of the emissive layer gradually. Similar phenomenon would also take place in devices with salts shortly after the bias was just applied since additional mobile ions accelerated extension of the doped layers. However, the EL emission was not bright enough for spectra fitting at the very early stage of operation and thus the later temporal evolution of the recombination zone in devices with salts was dominated by gradually enhanced electron injection. These results reveal that incorporating salts in the emissive layer significantly alters carrier balance of LECs. Utilizing salts of proper sizes would be beneficial in tailoring the recombination zone position to mitigate exciton quenching near the doped layers and to optimize the device efficiency. However, after reaching the maximum value, the EQE decreased with time when the device current was still increasing (cf. Figs. 3 and 6). It revealed that exciton quenching due to continuous extension of the doped layers deteriorated the device efficiency [19]. Dynamic doping profiles would be the obstacle to maintain the optimal operation condition. Techniques to fix the doping profiles by freezing ionic motion would be a feasible way to keep the optimized device efficiency during operation [43].

It is noted that temporal evolution trend of the EQE is different for LECs with and without salts (Fig. 6). The maximum EQE of all LECs reached shortly after the bias was applied. Then the EQE gradually decreased toward a steady-state value. However, the EQEs of the devices doped with salts approached steady-state values at ca. 200 min while the EQE of the neat-film device decreased more quickly to reach a steady-state value. Temporal evolution of the recombination zone shown in Fig. 8 can explain the difference in temporal evolution of EQE between the devices with and without salts. Initially, the recombination zone of the neat-film device (**N2**) was closest to the electrode (Fig. 8a). When the doped layer was growing, the distance between the doped layer and the recombination zone decreased rapidly and thus fastest decay rate in EQE for device **N2** could be expected initially. For devices doped with salts, devices **E2** and **O2** showed more off-centered recombination zone (Fig. 8b and e) and thus they exhibited faster decay rate in EQE as compared to devices **B2** and **H2**

(Fig. 6) for the same reason. With temporal evolution of EQE and recombination zone, we can only speculate that the decay rate of EQE is dependent on the initial recombination zone position. However, all devices showed similar steady-state EQEs (Fig. 6) while their stabilized recombination zone positions were different (Fig. 8). It implies that uneven p- and n-type doped layers may be formed finally in these devices such that the degree of exciton quenching is similar for all devices. Further studies will be required to clarify detailed effect of salt addition on growing of the doped layers. For instance, temporal evolution of p- and n-type doping front positions should be measured to determine accurate time-dependent distances between the recombination zone and the doped layers. However, these data can not be obtained by employing a technique based on optical interference since the doped layers are not emissive.

The photoluminescence quantum yield (PLQY) of the emissive layer would also be responsible for the trend in the device efficiency as the alkyl chain length of the added salt varied. To study this effect, we measured the PLQYs of the thin films of the emissive layers. The measured PLQYs of the emissive layers of the devices **N2**, **E2**, **B2**, **H2** and **O2** were 17%, 19%, 19%, 21% and 23%, respectively. Compared to the neat film of complex **1**, the PLQYs of the thin films of complex **1** doped with salts were enhanced due to reduced self-quenching effect. Measured PLQYs enhanced as the alkyl chain length of the added salt increased. It confirms that a larger molecular size of the doped salt separates the complexes and self-quenching is reduced. Therefore, intermolecular distance and carrier transport property of the complex film can be modified by salt addition. The maximal EQE can be estimated by $b\varphi/2n^2$, where b is the recombination efficiency (equal to unity for balanced carrier injection), φ is the PLQY of the emissive material and n is the refractive index of the glass substrate (the factor $1/2n^2$ is the light outcoupling efficiency of a bottom-emitting device) [5]. Estimated maximal EQEs of the devices **N2**, **E2**, **B2**, **H2** and **O2** were 3.74, 4.18, 4.18, 4.62 and 5.06%, respectively. The percentages of the measured EQEs (Table 1) as compared to the estimated maximal EQEs for the devices **N2**, **E2**, **B2**, **H2** and **O2** were calculated to be 49%, 61%, 78%, 68% and 47%, respectively. These ratios are strongly dependent on the initial recombination zone positions (Fig. 8). Device **B2** showed the most centered initial recombination zone and thus suffered the least exciton quenching, rendering the highest ratio in measured EQE with respect to the estimated maximal EQE. On the other hand, for devices **N2** and **O2** possessing significantly off-centered recombination zones, only half of the maximal EQEs were achieved due to severe exciton quenching. Compared to the neat-film device, the enhancement in device efficiency for the salt-doped device with poor carrier balance (device **O2**) mainly results from increased PLQY of the emissive layer. However, for the salt-doped device with good carrier balance (device **B2**), enhancement in PLQY of the emissive layer (only 12%) can not account for improvement in device efficiency as compared to the neat-film device (78%). These results reveal that carrier balance of the device rather than PLQY of the emissive layer dominates the device efficiency of the devices doped with salts.

The temporal evolution of the recombination zone also affect the turn-on time of LECs doped with salts. In a previously reported work [28], device response of LECs containing salts was slower when a salt with a longer alkyl chain length, which decreased the ionic mobility of the emissive layer, was used. However, the device turn-on time, which is defined as the time required to reach half of the maximal light output (before reaching the maximal light output), increased as the alkyl chain length of the added salt increased except for the devices **E2** (Table 2), which is not consistent with what was observed in Ref. [28]. As shown in Fig. 3, the times required for the current density of the device **E2** and **B2** to reach the maximum were similar. Thus, the ionic mobility of the device **E2** and **B2** was also similar. It revealed that the abnormal trend in turn-on times of the devices **E2** and **B2** would result from light-emitting properties rather than ionic conductivity issues. Since the turn-on time is defined as the time required to reach half of the maximal light output, it would be affected by exciton quenching near the electrode during operation. Exciton quenching in the device **E2** was more severe initially and then was gradually reduced when the recombination zone was moving toward the center of the emissive layer (Fig. 8b). Thus, the light output was quenched more significantly at the early stage of operation and the time to reach the light output maximum was delayed. On the other hand, the temporal recombination zone evolution of device **B2** (Fig. 8c) was closer to the center of the emissive layer. The time to reach half of the light output maximum was relatively unaffected by the exciton quenching effect, rendering a shorter turn-on time as compared to that of the device **E2**. Hence, the turn-on time of device **E2** would be similar to that of device **B2** if exciton quenching effect was absent. Both devices **E2** and **B2** should have faster device response than device **N2**. In the previous work of Ref. [28], the device thickness was relatively much thinner (ca. 100 nm) and exciton quenching was universally significant in all devices. Hence, the trend of device response perfectly aligned with the alkyl chain length of the added salts since differential quenching of light output was not significant in the devices under study. It is noted that as compared to the neat-film device, the devices doped with salts did not show significantly reduced turn-on times and these results are not consistent with those reported previously [28]. Recently, LECs based on $[Ir(ppy)_2(bpy)][PF_6]$ (where ppy is 2-phenylpyridine and bpy is 2,2′-bipyridyl) doped with salt additives $[NH_4][PF_6]$ and $K[PF_6]$ have also been reported to exhibit slower response than the undoped devices [29]. However, the devices doped with $Li[PF_6]$ showed significantly reduced turn-on times [29]. The cationic radii of NH_4^+, K^+ and Li^+ are 1.43, 1.33 and 0.87 Å, respectively [29]. These results are similar to those observed in our study, i.e. the salts with larger cations ($HMIMPF_6$ and $OMIMPF_6$) showed longer turn-on times while the salts with smaller cations ($EMIMPF_6$ and $BMIMPF_6$) exhibited faster device response (Table 1). Therefore, to reduce the turn-on time of LECs, the salts added should have small enough cations. This phenomenon may be related to the crystalline structure with intermediate-range order, i.e. about three complex lattices for

Ru complex, in spin-coated films [44]. These crystals may block moving of ions and affect dissociation of the salt with larger cations.

4. Conclusions

In summary, we have demonstrated enhancing efficiency of LECs by incorporating imidazole-based salts bearing various lengths of alkyl chains. The device current decreased monotonically with increasing alkyl chain length of the added salt while the device efficiency was nearly doubled as compared to that of the neat-film device when a salt with a proper alkyl chain length was employed. To shed light on the physical insights of the salt size on device performance, temporal evolution of the recombination zone for devices without and with salts were estimated by fitting the measured time-dependent EL spectra to the simulation model concerning microcavity effect. The extracted recombination zone of LECs moved toward the anode as the alkyl chain length of the added salt increased. It indicates that a larger salt size would relatively impede hole transport more significantly than electron transport. Therefore, the device efficiency of LECs can be optimized by incorporating a salt with a proper size to achieve centered recombination zone, which reduces exciton quenching near the doped layers.

Acknowledgement

The authors gratefully acknowledge the financial support from the National Science Council of Taiwan.

References

[1] Q. Pei, G. Yu, C. Zhang, Y. Yang, A.J. Heeger, Science 269 (1995) 1086.
[2] Q. Pei, Y. Yang, G. Yu, C. Zhang, A.J. Heeger, J. Am. Chem. Soc. 118 (1996) 3922.
[3] C.W. Tang, S.A. VanSlyke, Appl. Phys. Lett. 51 (1987) 913.
[4] J.K. Lee, D.S. Yoo, E.S. Handy, M.F. Rubner, Appl. Phys. Lett. 69 (1996) 1686.
[5] S. Bernhard, J.A. Barron, P.L. Houston, H.D. Abruña, J.L. Ruglovksy, X. Gao, G.G. Malliaras, J. Am. Chem. Soc. 124 (2002) 13624.
[6] J.D. Slinker, D. Bernards, P.L. Houston, H.D. Abruña, S. Bernhard, G.G. Malliaras, Chem. Commun. (2003) 2392.
[7] J.D. Slinker, A.A. Gorodetsky, M.S. Lowry, J. Wang, S. Parker, R. Rohl, S. Bernhard, G.G. Malliaras, J. Am. Chem. Soc. 126 (2004) 2763.
[8] A.B. Tamayo, S. Garon, T. Sajoto, P.I. Djurovich, I.M. Tsyba, R. Bau, M.E. Thompson, Inorg. Chem. 44 (2005) 8723.
[9] Q. Zhang, Q. Zhou, Y. Cheng, L. Wang, D. Ma, X. Jing, F. Wang, Adv. Funct. Mater. 16 (2006) 1203.
[10] H.-C. Su, F.-C. Fang, T.-Y. Hwu, H.-H. Hsieh, H.-F. Chen, G.-H. Lee, S.-M. Peng, K.-T. Wong, C.-C. Wu, Adv. Funct. Mater. 17 (2007) 1019.
[11] H.-C. Su, C.-C. Wu, F.-C. Fang, K.-T. Wong, Appl. Phys. Lett. 89 (2006) 261118.
[12] J.D. Slinker, J. Rivnay, J.S. Moskowitz, J.B. Parker, S. Bernhard, H.D. Abruña, G.G. Malliaras, J. Mater. Chem. 17 (2007) 2976.
[13] H.-C. Su, H.-F. Chen, F.-C. Fang, C.-C. Liu, C.-C. Wu, K.-T. Wong, Y.-H. Liu, S.-M. Peng, J. Am. Chem. Soc. 130 (2008) 3413.
[14] H.J. Bolink, E. Coronado, R.D. Costa, N. Lardiés, E. Ortí, Inorg. Chem. 47 (2008) 9149.
[15] L. He, L. Duan, J. Qiao, G. Dong, L. Wang, Y. Qiu, Chem. Mater. 22 (2010) 3535.
[16] H.-C. Su, Y.-H. Lin, C.-H. Chang, H.-W. Lin, C.-C. Wu, F.-C. Fang, H.-F. Chen, K.-T. Wong, J. Mater. Chem. 20 (2010) 5521.
[17] H.-C. Su, H.-F. Chen, Y.-C. Shen, C.-T. Liao, K.-T. Wong, J. Mater. Chem. 21 (2011) 9653.
[18] C.-T. Liao, H.-F. Chen, H.-C. Su, K.-T. Wong, J. Mater. Chem. 21 (2011) 17855.
[19] M. Lenes, G. Garcia-Belmonte, D. Tordera, A. Pertegás, J. Bisquert, H.J. Bolink, Adv. Funct. Mater. 21 (2011) 1581.
[20] H.-B. Wu, H.-F. Chen, C.-T. Liao, H.-C. Su, K.-T. Wong, Org. Electron. 13 (2012) 483.
[21] T. Hu, L. He, L. Duan, Y. Qiu, J. Mater. Chem. 22 (2012) 4206.
[22] R.D. Costa, E. Ortí, H.J. Bolink, F. Monti, G. Accorsi, N. Armaroli, Angew. Chem. Int. Ed. 51 (2012) 8178.
[23] C.-T. Liao, H.-F. Chen, H.-C. Su, K.-T. Wong, Phys. Chem. Chem. Phys. 14 (2012) 9774.
[24] H.-C. Su, H.-F. Chen, P.-H. Chen, S.-W. Lin, C.-T. Liao, K.-T. Wong, J. Mater. Chem. 22 (2012) 22998.
[25] Y.-P. Jhang, H.-F. Chen, H.-B. Wu, Y.-S. Yeh, H.-C. Su, K.-T. Wong, Org. Electron. 14 (2013) 2424.
[26] J.-S. Lu, J.-C. Kuo, H.-C. Su, Org. Electron. 14 (2013) 3379.
[27] S.T. Parker, J.D. Slinker, M.S. Lowry, M.P. Cox, S. Bernhard, G.G. Malliaras, Chem. Mater. 17 (2005) 3187.
[28] R.D. Costa, A. Pertegás, E. Ortí, H.J. Bolink, Chem. Mater. 22 (2010) 1288.
[29] Y. Shen, D.D. Kuddes, C.A. Naquin, T.W. Hesterberg, C. Kusmierz, B.J. Holliday, J.D. Slinker, Appl. Phys. Lett. 102 (2013) 203305.
[30] Y. Hu, J. Gao, Appl. Phys. Lett. 89 (2006) 253514.
[31] J.-H. Shin, N.D. Robinson, S. Xiao, L. Edman, Adv. Funct. Mater. 17 (2007) 1807.
[32] K. Matsumoto, R. Hagiwara, R. Yoshida, Y. Ito, Z. Mazej, P. Benkič, B. Žemva, O. Tamada, H. Yoshino, S. Matsubara, Dalton Trans. (2004) 144.
[33] G. Singh, A. Kumar, Indian J. Chem. A 47 (2008) 495.
[34] A.B. Pereiro, E. Tojo, A. Rodríguez, J. Canosa, J. Tojo, J. Chem. Thermodyn. 38 (2006) 651.
[35] T.-W. Wang, H.-C. Su, Org. Electron. 14 (2013) 2269.
[36] L.J. Soltzberg, J.D. Slinker, S. Flores-Torres, D.A. Bernards, G.G. Malliaras, H.D. Abruña, J.-S. Kim, R.H. Friend, M.D. Kaplan, V. Goldberg, J. Am. Chem. Soc. 128 (2006) 7761.
[37] G. Kalyuzhny, M. Buda, J. McNeill, P. Barbara, A.J. Bard, J. Am. Chem. Soc. 125 (2003) 6272.
[38] X. Liu, D. Poitras, Y. Tao, C. Py, J. Vac. Sci. Technol. 22 (2004) 764.
[39] I.H. Campbell, D.L. Smith, C.J. Neef, J.P. Ferraris, Appl. Phys. Lett. 72 (1998) 2565.
[40] W.K. Chan, P.K. Ng, X. Gong, S. Hou, Appl. Phys. Lett. 75 (1999) 3920.
[41] J. Kesters, T. Ghoos, H. Penxten, J. Drijkoningen, T. Vangerven, D.M. Lyons, B. Verreet, T. Aernouts, L. Lutsen, D. Vanderzande, J. Manca, W. Maes, Adv. Energy Mater. 3 (2013) 1180.
[42] S. van Reenen, P. Matyba, A. Dzwilewski, R.A.J. Janssen, L. Edman, M. Kemerink, Adv. Funct. Mater. 21 (2011) 1795.
[43] G. Yu, Y. Cao, M. Andersson, J. Gao, A.J. Heeger, Adv. Mater. 10 (1998) 385.
[44] D.R. Blasini, J. Rivnay, D.-M. Smilgies, J.D. Slinker, S. Flores-Torres, H.D. Abruña, G.G. Malliaras, J. Mater. Chem. 17 (2007) 1458.